22 MECHANISMS OF DEGRADATION OF PORTLAND CEMENT-BASED SYSTEMS BY SULFATE ATTACK

C.F. FERRARIS, J.R. CLIFTON, P.E. STUTZMAN and E.J. GARBOCZI
National Institute of Standards and Technology, Gaithersburg, MD, USA

Abstract
Although the chemical mechanisms of sulfate attack have been studied by many researchers, considerable disagreement exists over the mechanics of the associated expansion and cracking processes. Studies were carried out by exposing mortar and concrete specimens of different geometries (prisms, cylinders, and spheres) to sodium sulfate solutions with controlled pH (7,9,11). Relationships between the formation of reaction products and the expansion of portland cement mortars were investigated by identifying the reaction products present as a function of attack depth and amount of expansion. Simulation modeling based on a finite element approach is being performed to elucidate the mechanics of the cracking induced by sulfate attack.
Keywords: Sulfate attack, microstructure, mortar, environment influence

1. Introduction

A potentially significant degradation process for underground concrete vaults made for the disposal of low-level radioactive waste is sulfate attack [1]. In a previous paper [2], a model of the kinetics of sulfate attack of cement-based materials was described. Further studies have been carried out for the purpose of developing relationships among the formation of reaction products, the depth of sulfate penetration, and the amount of expansion. Simulation modeling, based on a finite element approach, is also being performed to elucidate the mechanics of expansion and cracking. In the present paper, results of experimental studies and simulation modeling of the mechanics of expansion and cracking during sulfate attack are given.

Mechanisms of Chemical Degradation of Cement-based Systems. Edited by K.L. Scrivener and J.F. Young. Published in 1997 by E & FN Spon, 2-6 Boundary Row, London SE1 8HN. ISBN: 0419215700.

2. Experimental Studies and Results

2.1. Influence of sodium sulfate concentration and pH

The focus of NIST sulfate attack experimental is the determination of the influence of the environment and the mechanisms of the deterioration. The variables in the experimental design were:

- pH of the controlled-pH sulfate solutions: 7, 9 and 11
- sulfate solution concentrations: 0 to 10 % sodium sulfate solution (by weight)
- C_3A content of the cements: 2.8, 4, 6, 8, 11.1 and 12.8 % (ASTM C150 [3])

All the tests were performed using mortar prism specimens (25 mm x 25 mm x 279 mm). The mortar mixtures were prepared according to ASTM C109 [4] specifications. Three cements were blended to vary the C_3A content (ASTM C150 [3]) of the cement used in the sample preparation:

- Cement 1: 2.7 % C_3A
- Cement 2: 11.1 % C_3A
- Cement 3: 12.8 % C_3A

Cement 1 was mixed with either Cement 2 or Cement 3 to prepare "mixed" cements with 4, 6, and 8% C_3A content.

The pH of the solution in which the samples were placed was controlled using an automatic burette that added sulfuric acid (1 N) when the pH rose above a preset value [5]. In a separate experiment, the uncontrolled pH of the solution rose to 12 in a few days [5]. The changes in length of each specimen was monitored until disintegration of the specimen occurred. Each value reported is the average of 3-7 bars. Figure 1 shows the results obtained.

All the factors examined seem to have an effect on the rate of deterioration of the samples as measured by the time to reach 0.1% elongation. This criterion was selected, instead of 0.5% as reported elsewhere [5], because most of the samples had already disintegrated before they had expanded by even 0.3%. All specimens were mortar prisms 25 mm x 25 mm x 276 mm. The mix design was as described in ASTM C109 [4] . In Figure 1, a shorter time indicates a faster expansion of the specimen. The C_3A content is the main factor affecting the rate of expansion (Figure 1b). When the solution pH was not controlled, but instead the solution was changed each time a measurement was made according to ASTM C1012 [6], a longer time to reach 0.1% expansion was required, i.e., the deterioration was slower (Figure 2). Therefore, a controlled pH environment allows a faster assessment of the sulfate resistance as was also determined previously [5]. As would be predicted, a higher concentration of sodium sulfate in the solution led to faster expansion of the specimens. This series of tests confirms the importance of sodium sulfate concentration and pH on service life.

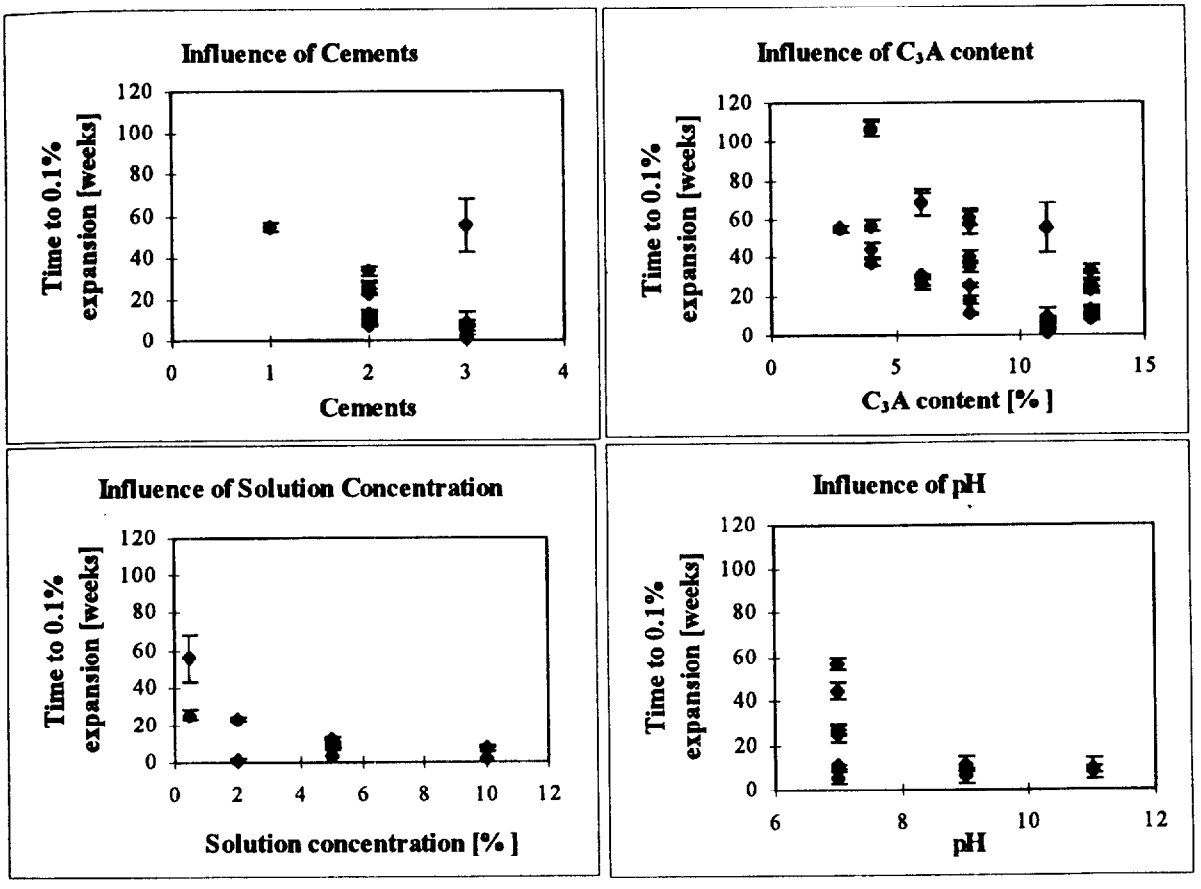

Figure 1: Influence of various factors on the time in weeks to reach 0.1% expansion. In the lower graphs, the data shown are with all three cements. (error bars are ± σ)

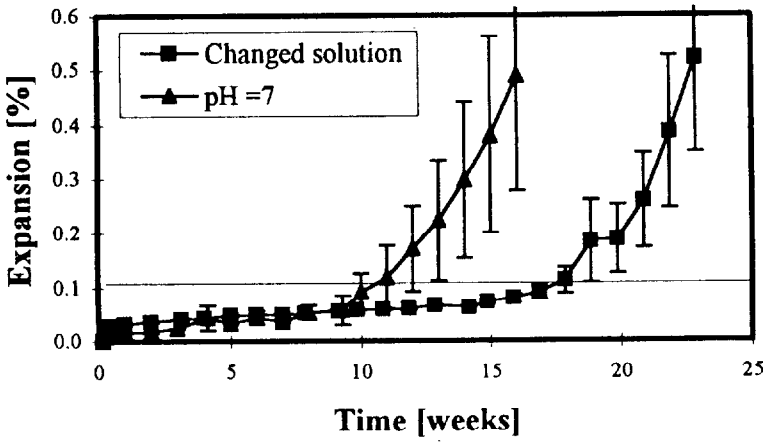

Figure 2: Expansion versus time in solutions in which the pH was a) controlled or b) uncontrolled. The initial concentration of sodium sulfate solution was 5%.(Cement 3 used) (error bars are ± σ)

2.2. Microstructure

The deterioration mechanism was studied by analyzing the microstructures of the specimens, the composition of the reaction products, and observing the form of distress. Samples were taken for X-ray powder diffraction (XRD) analysis at selected times during the tests shown in Figure 2, to provide information on the changes in crystalline products as a function of depth and time. A sliced cross section was sampled as follows: the outer 3 mm, labeled as "outer", the next 3 mm, labeled as "inner", and the center of the section, labeled as "core". Each sample was gently crushed and sieved through a 100 mesh (150 μm, ASTM E 11 [7]) screen to remove the bulk of the quartz sand. The hardened cement paste powder was stored in a desiccator under a constant relative humidity of 33% to prevent dehydration of the calcium aluminosulfates. The powdered samples were analyzed within 24 hours to minimize influence of carbonation.

Scanning electron microscopy using backscattered electron and X-ray imaging of resin-impregnated, polished sections provide information on: phases, phase composition, textural and morphological relationships, and porosity. The resin impregnation was carried out as follows. Sections cut at selected time intervals throughout the experiment were placed in ethanol to stop hydration, and then placed in a low-viscosity resin to impregnate the microstructure without drying and to minimize the possibility of inducing drying shrinkage cracks. The resin was cured at 60 °C for 24 hours, and the samples polished with a 0.25μm diamond paste on a lap wheel. The surface was coated with a thin layer of carbon to provide the conductive surface necessary for SEM imaging.

The following observations were made. First, the sulfur distribution determined by X-ray imaging indicated a high concentration to about 2 mm from the surface relative to the control samples, cured in limewater. This corresponds to a gypsum-rich zone in the outer microstructure. The transition between gypsum-rich paste and paste beyond this zone is quite abrupt, and in severely-damaged mortar bars, the interface separates an outer region of coarse cracking typically parallel to the mortar bar surface, and the interior region which contains inter-aggregate cracking. The core at later ages is not devoid of gypsum or ettringite, however, as will be noted in the discussion of the X-ray diffraction (XRD) results. Quantitative energy dispersive X-ray spectrometry (EDS) analysis of sodium levels in the calcium silicate hydrate (C-S-H) showed high concentration in the outer 200 μm while sodium was not detected in C-S-H at greater depths. Calcium depletion was observed in the outer C-S-H as calcium/silicon ratios are markedly lower in the sulfate-exposed mortars relative to the control mortar. This ratio increases to the value of the control mortar around one millimeter of depth. The outer (less than 250 μm) microstructure of the sulfate-exposed specimen relative to the control (equal age in their respective solutions) exhibits scaling and appears to be almost completely devoid of unhydrated cement particles and overall darker (Figure 3). This darkening of the paste may originate from two sources: compositional changes (as in the leaching of Ca), or an overall increase in porosity. These features were also observed by Taylor [8].

Second, after three days, the outer layer contains ettringite, gypsum, monosulfate, and gypsum. Void space appears to be "filled" with reaction product. In some cases replacement of calcium hydroxide with gypsum and large deposits of ettringite are

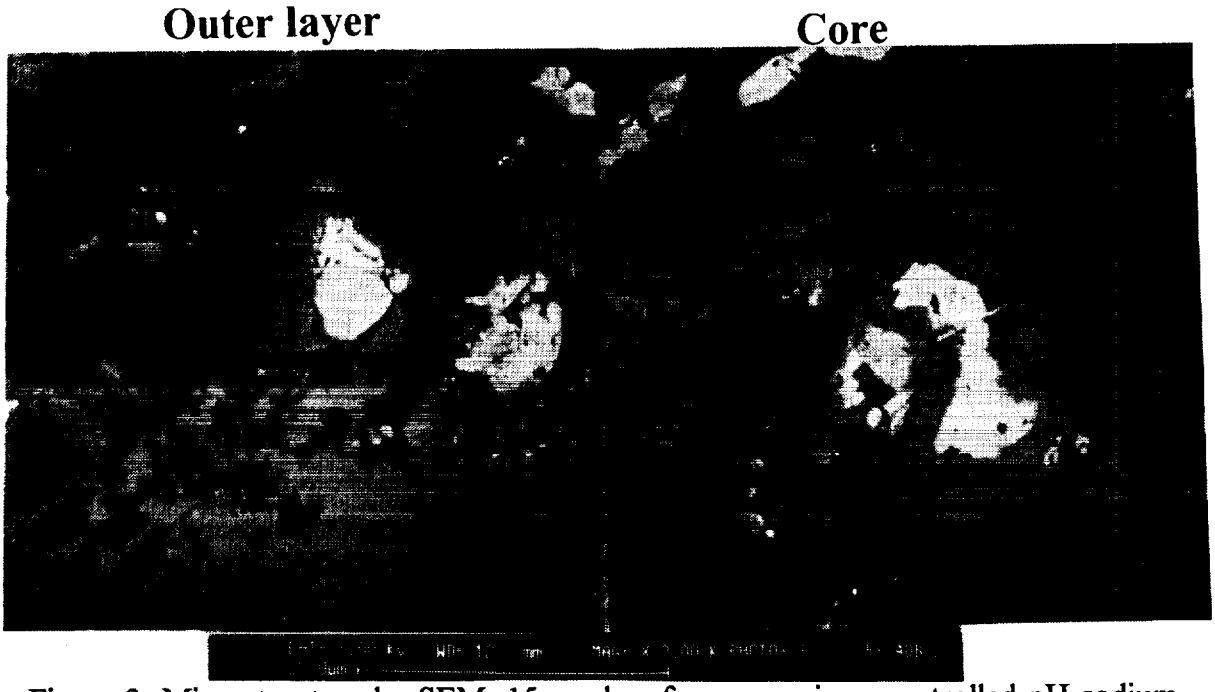

Figure 3: Microstructure by SEM; 15 weeks of exposure in uncontrolled pH sodium sulfate (5% by weight) solution.

common. In contrast, the inner layer and core sampled at the same time show the presence of calcium hydroxide, monosulfate and traces of ettringite. Massive deposits of ettringite are not found in the core until late stages of testing, after the rapid increase in expansion.

Third, at 28 days, gypsum and ettringite were detected throughout the specimen, while the monosulfate appears to decrease. Gypsum and ettringite increase with age at all depths while calcium hydroxide decreases, though the changes in phase proportions do not appear to be as great as in the outer few millimeters of the specimen.

2.3. Specimen shape and spalling

Three specimen geometries were used: cylinders (various diameters), spheres and prisms. The cylinders had diameters of 25, 50 and 75 mm. To determine if one of the leading mechanisms of deterioration by the sulfate is governed by the transport of the sulfate ions into the specimen, the cylinders were capped at the ends so that the penetration of the sodium sulfate was only perpendicular to the cylinders main axis. It was observed that the larger diameter cylinders expanded more slowly than the smaller diameter cylinders (Figure 4). This observation suggests that the transport rate of sulfate ions into the material governs the deterioration. Companion prisms (25mm x25 mm x 279mm) tested at the same time expanded like the 25mm diameter cylinders, confirming that the size and not the shape was the important factor in the time scale of the expansion due to sulfate attack, although the cracking pattern was different. During this test, it was observed that the outer layer of the 75-mm-diameter specimen

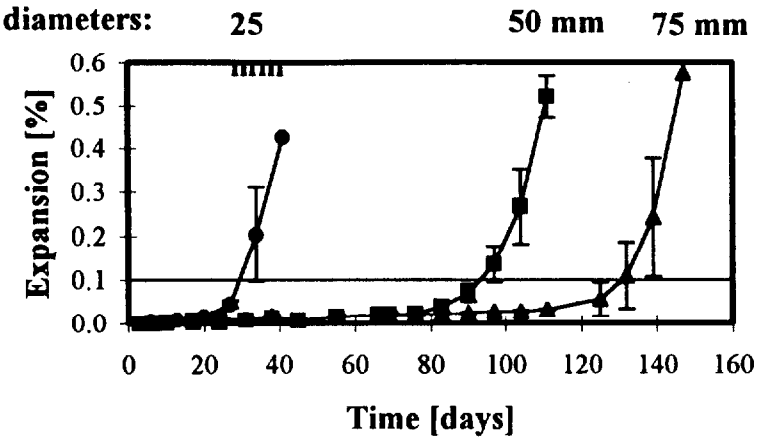

Figure 4: Influence of the diameter on the expansion of the cylinders. Type I Portland cement was used.

was peeling like an onion (several layers). To determine the influence of aggregate size on the depth of spalling and simultaneously avoid end effects, spheres were cast of mortar (2.36 mm maximum diameter sand), cement paste, and concretes (12-19 mm or 4-8 mm diameter coarse aggregates). It was observed that the samples peeled like an onion (successive layers) for the mortar and the finer concrete after 3 and 5 months, respectively, while the cement paste and the coarser aggregate concretes did not show cracks after 9 months. The thickness of the skin did not reflect the different size of the aggregates used, probably because it depends more on the paste-rich outer layer that forms on any sample cast in a mold.

3. Discussion of mechanics of expansion and cracking

The kind of cracking seen in the sulfate-attacked specimens was observed to depend on the specimen geometry. For example, the stress concentrations introduced by the sharp edges on the sides and ends of the prisms and the ends of the cylinders led to cracking along these edges first, which tended to dominate the subsequent random surface cracking and spalling. The spheres that showed cracking had random surface cracking only, followed by spalling. This has led to an attempt to use elasticity theory and finite element modeling to try to understand the mechanics of the degradation process as modified by sample geometry.

The conceptual model is the following. Sulfate ions enter the material and react with various phases of the mortar, which then grow in size, inducing stresses throughout the specimen. The specimen is modeled as a composite of expansive inclusions in an elastic matrix. The inclusions are modeled as having an intrinsic strain ε^{o}_{j}, so that the stress σ_i in the inclusions is given by [9]

$$\sigma_i = C_{ij} (\varepsilon_j - \varepsilon^{o}_{j}). \qquad (1)$$

where C_{ij} is the elastic tensor and ε_j is the strain. In this case, the diagonal components of the ε^{o}_{j} matrix are positive and identical, allowing for a pure expansion only.

A recent effort at analytical modeling [10] of alkali-silica reaction, which in terms of elasticity theory is similar mathematically, gave a uniform value of ε^o_j for a given surface layer. If this idea is applied to sulfate attack in a macroscopic way, the entire surface of the sample would have, down to the depth of the sulfate attack, to have a positive intrinsic strain and thus tend to expand. This however results in compressive-only stresses in the outer layers, since the expansive layer remains in compression, due to the unreacted layers underneath that restrain the expansion so that $\varepsilon < \varepsilon^o_j$, resulting in a compressive stress according to eq. (1). Uniform compressive stress in the layer will not result in the kinds of surface cracking seen experimentally. This analysis seems to rule out any exact mathematical analysis of the mechanics, and thus suggests that a random model must be used.

It is necessary to go back to the expansive inclusion model mentioned above. In this model, any surface layer will contain both matrix and inclusions. The inclusions will still be in compression, due to the restraining matrix, but the matrix will be in tension, in order to balance the expansive inclusions and result in an overall average stress of zero, since the samples can freely expand. These random tension fields can result in the kind of random cracking seen experimentally. The causes of the delamination seen are more subtle, and are clearly related to the cement paste "skin" effect arising from the mold. It would be interesting to redo the cylinder experiments with cores, so there is no possible effect from the mold.

A numerical solution of the random inclusion model can be attempted by building up samples of the appropriate geometry out of cubic pixels, and then applying a 3-D finite element model [11]. A cube of material with a volume fraction of about 5% expansive material was generated, and then the appropriate sample was "cut out", exposing some of the expansive sites on the surface. Only these sites are allowed to grow, simulating a fairly early stage of sulfate attack where the sulfate ions have not penetrated all the way through the sample. Solving the elastic equations will then induce stresses mainly in the sample surface. The principal stresses for each pixel were calculated by diagonalizing the average stress matrix per pixel. Only preliminary results are available at present, for the case of a cylinder whose entire surface was open to sulfate penetration. In this case, random tensile stress fields were seen over the sample surface, and somewhat higher principal tensile stresses were seen at the cylinder ends, a result of the stress concentration from the cylinder edges. These preliminary results seem to confirm the ideas discussed above, although the role of creep in response to these localized stresses needs also to be considered.

4. Conclusions

The following conclusions can be drawn:

- Environmental conditions such as pH of the solution and the sulfate concentration played an important role in the rate of expansion of the cement-based specimens
- The C_3A content of cements also influenced the rate of deterioration of the specimen
- Massive deposits of ettringite appeared in the core only at late stages of testing, after a large amount of expansion.

- The outer paste (near the mold surface) present in a molded specimen plays an important role in the deterioration due to sulfate attack
- The feasibility of finite element modeling of the expansion and cracking caused by sulfate attack was demonstrated

5. Acknowledgments

This work was sponsored by the "High Performance Construction Materials" program at NIST, by the Nuclear Regulatory Commission and the National Science Foundation Center for Science and Technology of Advanced Cement-Based Materials (ACBM). We would like to thank M. Yang for producing the finite element results, John Winpigler and Frank Davis for performing some of the experimental measurements.

6. References

1. Clifton, J.R., Knab, L.I., (1989), *Service Life of Concrete*, NIST report #89-4086, National Institute of Standards and Technology, Gaithersburg MD 20899
2. Pommersheim, J.M., Clifton, J.R., (1994), Expansion of Cementitious Materials Exposed to Sulfate Solutions, *Mat. Res. Soc. Symp. Proc.* Vol 333, pp 363-368.
3. ASTM (1994), *Standard Specification for Portland Cement*, ASTM designation C150-94, Annual Book of ASTM Standards Vol. 04.02.
4. ASTM (1994), *Standard Test Method for Compressive strength of Hydraulic Cement Mortars (using 2-in. or 50-mm cube Specimens*, ASTM designation C109-93, Annual Book of ASTM Standards Vol. 04.02.ASTM C109
5. Brown, P.W., (1981), An Evaluation of the Sulfate Resistance of Cements in a controlled Environment. *Cement and Concrete Research*, Vol. 11 pp. 719-727
6. ASTM (1994), *Standard Test Method for Length Change of Hydraulic-Cement Mortars Exposed to a Sulfate Solution*, ASTM designation C1012-89, Annual Book of ASTM Standards Vol. 04.02.
7 ASTM (1995), *Standard Specification for Wire Cloth and Sieves for Testing Purposes*, ASTM designation E 11-95, Annual Book of ASTM Standards Vol. 04.02
8. Taylor, H.F.W., (1993) Sulfate Reactions in Concrete-Microstructural and Chemical Aspects, *Cement and Technology*, ed. by Gartner, E. M. and Uchikawa H., Ceramic Transactions vol. 40
9. Cook, R.D., Malkus, D.S., Plesha M.E., (1989) *Concepts and Applications of Finite Element Analysis*, J, Wiley and Sons, New York 3rd ed
10. Goltermann,P., (1994) Mechanical predictions on concrete deterioration. Part I: Eignestresses in concrete, *Amer. Conc. Inst. Mat. Journal* vol. 91, pp. 543-550
11 Garboczi, E.J., Day, A.R., (1995), An algorithm for computing the effective linear elastic properties of heterogeneous materials: Three-dimensional results for composites with equal phase Poisson ratios, *J. Mech. Phys. Sol.*, vol. 43, 1349-1362